Mineralogy and Petrology (2007) 89: 133–158
DOI 10.1007/s00710-006-0140-x
Printed in The Netherlands

Mineralogy and Petrology

The origin of rutile-ilmenite aggregates ("nigrine") in alluvial-fluvial placers of the Hagendorf pegmatite province, NE Bavaria, Germany

H. G. Dill, F. Melcher, M. Füßl, and **B. Weber**

Federal Institute for Geosciences and Natural Resources, Hannover, Germany

Received September 6, 2005; revised version accepted March 28, 2006

Editorial handling: J. G. Raith

Summary

Titanium placer deposits occur in alluvial-fluvial drainage systems which dissect Moldanubian gneisses intruded by Late Variscan pegmatites (Hagendorf province) in southern Germany. Based upon their texture (zonation, exsolution lamellae, intergrowth), microchemical data (Nb, Cr, Ta, V, Fe, W, Sn) and mineral inclusions, two major grain types of intergrown rutile and ilmenite have been established. Grains of type A are always zoned and consist of rutile cores enveloped by ilmenite containing small inclusions of wolframite. A core-rim transition zone is characterized by complex relations of rutile and ilmenite, with rutile lamellae being rich in Nb, V and Fe. Types B1 and B2 aggregates consist of ilmenite with lamellae of niobian rutile and/or ilmenorutile, and additionally have inclusions of ferrocolumbite, pyrochlore, betafite, sphalerite, pyrrhotite and Fe oxides. Such grain types featuring an intimate intergrowth of rutile and ilmenite were called nigrine. Type-C grains are quite similar in their morphological appearance but consist of W-enriched rutile devoid of mineral inclusions and reaction products. Pseudorutile and leucoxene replacing minerals of the nigrine aggregates are presumably caused by supergene alteration under fluctuating redox conditions. Phosphate and aluminum remobilized by supergene processes led to the formation of hydrous Ti-rich phases containing Al, P and Fe. High Nb and W concentrations in nigrine aggregates and in rutile type C may be taken as a marker for highly differentiated granites or pegmatites. This has implications for both, heavy-mineral-based provenance analysis and stream sediment exploration.

Introduction

According to *Clark* (1993), "nigrine" (also: Eisenrutil, iron-rutile) is a variety of rutile. Nigrine is described either as black ferruginous rutile that is homogeneous on a microscopic scale (*Ramdohr*, 1975), or as ilmenite pseudomorphosed by rutile (*Strübel* and *Zimmer*, 1982). The Latin word "nigrum" connotes a black mineral color and immediately directs thoughts to the most striking feature common to all these Ti heavy mineral aggregates, the dull black luster, by which they may easily be recognized in stream sediments. To avoid confusion, in the present study the term nigrine is used, without placing it in inverted commas, to describe aggregates of various Ti oxide minerals, including rutile and ilmenite, intimately intergrown with each other. The term is used irrespective of their composition and the quantity.

From the Pleystein area in NE Bavaria, Germany (Fig. 1), nigrine forming grains up to 2.5 cm in diameter was reported from alluvial-fluvial placer deposits by *Strunz* in 1961 (Fig. 2a–d). As he could not avail of any detailed analyses then, the author suspected cassiterite and rutile to be the main constituents of the placer deposits. Complex Ti oxide aggregates like those from SE Germany were also recorded from placer deposits elsewhere in the world, e.g., from Sierra Leone by *Raufuss* (1973) and from Malawi by *Bloomfield* (1958) and *Coakley* and *Mobbs* (2001). None of the papers quoted above reports on the complex nature of the placer mineral aggregates. Textural relationships, such as exsolution lamellae, grain size, intergrowth textures, mineral inclusions, the concentrations of certain trace elements, e.g., Cr, V and Nb, may fingerprint the formation of nigrine and whether it might be feasible for an industrial use (*Chernet*, 1999a, b). Information

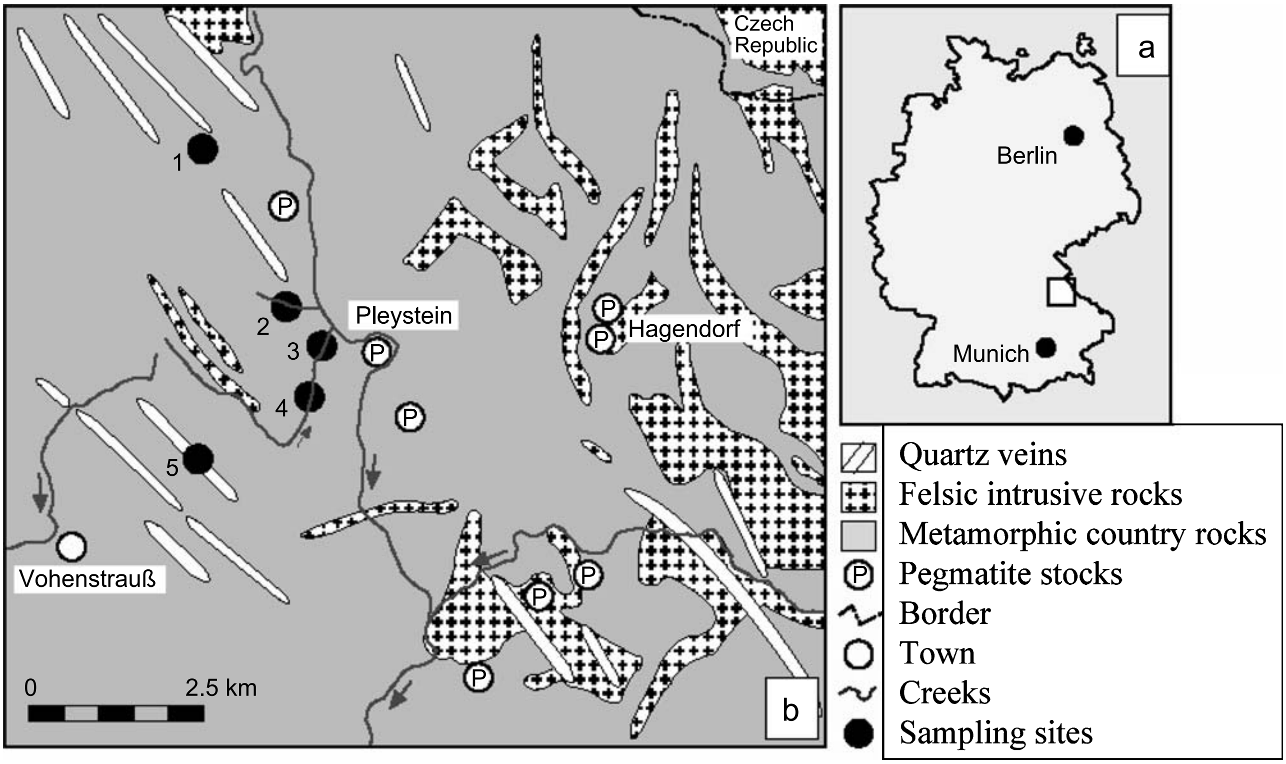

Fig. 1. Sketch map showing (**a**) the position of the study area in NE Bavaria, Germany and (**b**) the regional geology (modified after *Forster*, 1965). Sampling sites: *1* Steininger Loh, *2* Zollgraben, *3* Pingermühle, *4* Pflaumbach, *5* Weißenstein

Table 1. *Representative electron microprobe analyses of ilmenite and rutile varieties in grain types A to C from placer and bedrock*

Sample	7134/1	7193/4	7134/2	7194/4	7135	7193/3	7134/2	7194/1	7194/4	7167	7134/1	7193/4	7194/3
Location	Pingermühle (Zottbach)	Zollgraben	Pingermühle (Zottbach)	Iglasreuth Tirschenreuth	Pleystein (bedrock)	Zollgraben	Pingermühle (Zottbach)	Iglasreuth Tirschenreuth	Iglasreuth Tirschenreuth	Pleystein	Pingermühle (Zottbach)	Zollgraben	Iglasreuth Tirschenreuth
Analysis#	42	53	6	70	13	12	5	18	65	6	47	34	36
Grain type	A	A	B1	B2	A	A	B1	B2	B2	C	A	A	B2
Mineral	ilmenite	ilmenite	ilmenite	ilmenite	rutile (Nb)	rutile (Nb)	rutile (Nb)	rutile (Nb)	rutile (Nb)	rutile (W)	rt	rt	rt
TiO_2	52.38	52.85	49.30	51.29	89.39	87.78	85.53	66.87	95.70	93.22	98.17	98.19	98.80
Fe_2O_3	0.67	0.40	6.27	1.33									
FeO	45.33	44.95	41.71	43.48	2.79	2.94	4.20	6.85	0.65	2.07	0.30	0.24	0.38
MnO	1.17	2.21	2.34	2.16	bdl	0.07	0.03	0.02	bdl	bdl	bdl	bdl	0.04
Nb_2O_5	0.19	0.09	0.28	0.20	4.55	6.49	7.54	20.76	1.87	0.30	0.79	0.21	0.66
Ta_2O_5	bdl	0.04	bdl	0.04	0.39	0.38	0.56	1.18	0.03	bdl	bdl	bdl	0.04
Sc_2O_3	bdl	bdl	0.02	bdl	0.03	bdl	bdl	bdl	0.02	0.02	bdl	bdl	bdl
V_2O_3	0.18	0.27	0.29	0.34	1.38	1.38	0.68	2.62	0.95	1.06	0.91	0.69	0.45
Cr_2O_3	0.03	0.02	bdl	0.03	0.25	0.44	bdl	0.51	0.17	0.04	0.08	0.07	bdl
Al_2O_3	bdl	bdl	bdl	bdl	0.11	0.13	0.05	0.20	0.12	bdl	0.04	0.03	bdl
MgO	0.46	0.24	0.08	0.37	bdl	0.02	bdl	bdl	bdl	bdl	bdl	0.04	bdl
SiO_2	0.03	0.05	0.05	bdl	bdl	bdl	0.02	0.03	0.02	0.03	0.02	bdl	bdl
NiO	bdl	bdl	0.02	bdl	bdl	bdl	bdl	bdl	bdl	0.02	bdl	bdl	bdl
SnO	bdl	bdl	bdl	bdl	bdl	bdl	0.11	bdl	bdl	bdl	0.03	bdl	bdl
WO_3	bdl	bdl	bdl	bdl	1.37	0.50	0.31	1.33	0.14	4.87	0.04	bdl	bdl
PbO	bdl	bdl	bdl	bdl	bdl	bdl	0.19	bdl	bdl	0.11	bdl	bdl	bdl
Total	100.45	101.12	100.35	99.24	100.26	100.13	99.22	100.38	99.66	101.71	100.37	99.46	100.37
Ti	1.974	1.983	1.875	1.961	1.848	1.821	1.806	1.480	1.941	1.900	1.965	1.980	1.977
Fe^{3+}	0.026	0.014	0.239	0.050									
Fe^{2+}	1.900	1.874	1.758	1.848	0.064	0.068	0.099	0.169	0.015	0.047	0.007	0.005	0.009
Mn	0.050	0.094	0.100	0.092		0.002	0.001	0.000					0.001
Nb	0.004	0.002	0.007	0.005	0.057	0.081	0.096	0.276	0.023	0.004	0.009	0.003	0.008
Ta		0.001		0.001	0.003	0.003	0.004	0.009	0.000				0.000
Sc			0.001		0.001				0.000	0.000			
V	0.008	0.010	0.012	0.014	0.030	0.031	0.015	0.062	0.021	0.023	0.019	0.015	0.010
Cr	0.001	0.001		0.001	0.006	0.010		0.012	0.004	0.001	0.002	0.001	
Al					0.004	0.004	0.002	0.007	0.004		0.001	0.001	
Mg	0.034	0.018	0.006	0.028		0.001						0.001	
Si	0.001	0.003	0.002				0.001	0.001	0.000	0.001	0.001		
Ni			0.001							0.000			
Sn							0.001				0.000		
W					0.010	0.004	0.002	0.010	0.001	0.034	0.000		
Pb							0.001			0.001			
Total Cat	4.000	4.000	4.000	4.000	2.021	2.023	2.028	2.027	2.008	2.011	2.005	2.007	2.004

Cations are calculated on the basis of 6 (ilmenite) and 4 (rutile) oxygens; elements sought for, but not detected are U, P, Na, S, Ca; *bdl* below detection limit. Fe^{3+} and Fe^{2+} in ilmenite calculated using 4 cations

Table 2. *Representative electron microprobe analyses of mineral phases included in rutile and ilmenite, and average analyses of alteration products*

Sample	7134/2	7194/1	7134/1	7194/1	7134/2	7134/2	7134/2	7134/2	7193/1	7194/3	7134/1	7193	7194
Location	Pingermühle (Zottbach)	Iglasreuth Tirschenreuth	Pingermühle (Zottbach)	Iglasreuth Tirschenreuth	Pingermühle (Zottbach)	Pingermühle (Zottbach)	Pingermühle (Zottbach)	Pingermühle (Zottbach)	Zollgraben	Iglasreuth Tirschenreuth	Pingermühle (Zottbach)	Zollgraben	Iglasreuth Tirschenreuth
Analysis#	17	10	246	9	9	34	35	13	312–316	43–45			
Grain type	B1	B2	A	B2	B1	B1	B1	B1	A	B2	A	A	B2
N						2			5	3	14	26	9
Mineral	columbite	columbite	wolframite	wolframite	pyrochlore	betafite	altered betafite	magnetite	leucoxene?	leucoxene?	pseudorutile	pseudorutile	pseudorutile
Na_2O	bdl	bdl	bdl	bdl	bdl	1.29	0.08		bdl	bdl	bdl	bdl	bdl
MgO	0.26	0.50	0.98	0.58	bdl	bdl	bdl	0.03	0.06	0.12	0.52	0.22	0.15
Al_2O_3	0.03	bdl	bdl	0.05	0.03	0.10	2.23	0.02	8.45	6.09	0.07	0.09	0.03
SiO_2	0.10	0.06	bdl	bdl	0.29	0.09	4.68		0.49	0.71	0.03	0.03	bdl
P_2O_5	bdl	bdl	bdl	bdl	bdl	bdl	3.02		3.46	4.15	bdl	bdl	bdl
SO_2	bdl	bdl	bdl	bdl	bdl	bdl	0.07		0.09	bdl	bdl	bdl	bdl
CaO	0.60	0.83	bdl	bdl	17.91	15.38	0.36		0.28	0.05	bdl	bdl	bdl
Sc_2O_3	1.07	bdl	0.15	bdl	0.03	bdl	0.04		0.05	0.32	bdl	bdl	bdl
TiO_2	5.96	8.19	bdl	bdl	5.12	17.26	20.87	3.22	76.38	76.70	57.56	59.01	57.62
V_2O_3	0.04	0.22	bdl	0.29	0.04	0.08	0.18	0.17	0.53	0.62	0.28	0.32	0.29
Cr_2O_3	bdl	0.05	bdl	0.09	0.03	bdl	0.06	0.03	0.19	bdl	0.03	bdl	bdl
MnO	3.54	2.43	1.72	1.99	0.16	0.09	0.10	0.09	0.02	0.06	1.14	2.44	3.64
FeO (tot)	16.89	17.93	24.28	21.20	1.37	0.68	4.07	90.12	2.54	2.00	37.00	34.70	33.29
NiO	bdl	bdl	bdl	bdl	0.03	bdl	bdl		bdl	bdl	bdl	bdl	bdl
Nb_2O_5	69.76	64.55	0.66	6.51	74.13	32.14	42.72		0.15	0.16	0.25	0.23	0.23
SnO	0.14	bdl	bdl	bdl	0.05	0.29	0.27		bdl	bdl	bdl	bdl	bdl
Ta_2O_5	2.58	2.22	bdl	bdl	2.27	4.28	13.61		bdl	bdl	bdl	bdl	bdl
WO_3	0.69	4.71	70.43	62.89	0.40	0.60	bdl		bdl	bdl	bdl	bdl	bdl
PbO	bdl	bdl	bdl	bdl	0.30	1.00	0.99		bdl	bdl	bdl	bdl	bdl
UO_2	bdl	bdl	bdl	bdl	0.18	29.11	3.48		bdl	bdl	bdl	bdl	bdl
Sum	101.72	101.75	98.73	94.37	102.39	102.42	96.85	93.67	92.88	91.06	97.05	97.26	95.37
Na						0.178	0.010						
Mg	0.084	0.163	0.073	0.044				0.013	0.002	0.005	0.051	0.020	0.015
Al	0.009			0.003	0.002	0.008	0.160	0.007	0.280	0.206	0.005	0.007	0.003
Si	0.021	0.013			0.015	0.007	0.285		0.014	0.020	0.002	0.002	
P							0.156		0.082	0.101			
S							0.004		0.002				
Ca	0.141	0.194			1.002	1.178	0.024		0.008	0.002			
Sc	0.204		0.007		0.001		0.002		0.001	0.008			

(*continued*)

Table 2 (*continued*)

Sample	7134/2	7194/1	7134/1	7194/1	7134/2	7134/2	7134/2	7134/2	7193/1	7194/3	7134/1	7193	7194
Location	Pingermühle (Zottbach)	Iglasreuth Tirschenreuth	Pingermühle (Zottbach)	Iglasreuth Tirschenreuth	Pingermühle (Zottbach)	Pingermühle (Zottbach)	Pingermühle (Zottbach)	Pingermühle (Zottbach)	Zollgraben	Iglasreuth Tirschenreuth	Pingermühle (Zottbach)	Zollgraben	Iglasreuth Tirschenreuth
Analysis#	17	10	246	9	9	34	35	13	312–316	43–45			
Grain type	B1	B2	A	B2	B1	B1	B1	B1	A	B2	A	A	B2
N						2			5	3	14	26	9
Mineral	columbite	columbite	wolframite	wolframite	pyrochlore	betafite	altered betafite	magnetite	leucoxene?	leucoxene?	pseudorutile	pseudorutile	pseudorutile
Ti	0.976	1.348			0.201	0.928	0.956	0.745	1.618	1.651	2.832	2.907	2.895
V	0.007	0.039		0.012	0.002	0.005	0.009	0.041	0.012	0.014	0.015	0.017	0.015
Cr		0.009		0.003	0.001		0.003	0.006	0.004		0.001		
Mn	0.653	0.451	0.073	0.086	0.007	0.005	0.005	0.024	0.001	0.002	0.063	0.138	0.206
Fe^{3+}								14.439			2.024	1.875	1.859
Fe^{2+}	3.078	3.282	1.019	0.909	0.060	0.040	0.207	8.725	0.060	0.048	0.000	0.027	0.000
Ni					0.001								
Nb	6.873	6.387	0.015	0.151	1.750	1.039	1.176		0.002	0.002	0.007	0.006	0.007
Sn	0.014				0.001	0.009	0.007						
Ta	0.153	0.132			0.032	0.083	0.225						
W	0.039	0.267	0.916	0.836	0.005	0.011							
Pb					0.004	0.019	0.016						
U					0.002	0.463	0.047						
Total Cat	12.265	12.303	2.124	2.087	3.084	3.510	3.245	24.000	2.090	2.060	5.000	5.000	5.000
Oxygen	24	24	4	4	6	7	7	32	4	4	9	9	9

bdl Below detection limits; *N* number of analyses used to calculate average
High analytical totals in small grains are due to excitation from ilmenite

contained in nigrine from alluvial-fluvial placers is also of importance for sedimentologists for tracking back these heavy minerals to their provenance (*Morton*, 1984, 1985; *Dill*, 1998; *Zack* et al., 2002, 2004). The scope of the present study is to give an answer to these questions by providing mineralogical and chemical information on a detrital Ti mineralization genetically related to the emplacement of pegmatites.

Methodology

The coarse-grained "black sands" may be recovered by simple grab sampling and panning (Fig. 2c, d). The heavy minerals (density $>2.9\,g/cm^3$) were extracted from the 63–200 μm fractions by Na-polywolframate, a non-toxic heavy liquid. Grains mounted on a glass disk were identified and quantified under the petrographic microscope counting between 200 and 300 grains per sample. Examination of thin sections and X-ray diffraction analysis of particles larger than 200 μm supplemented the petrographic studies. Emphasis was placed on the study of polished sections under reflected light, in combination with electron microprobe analysis to identify the textural features and chemical composition, respectively. Electron microprobe analyses were carried out using a CAMECA SX100 equipped with five wavelength-dispersive spectrometers and a Princeton Gamma Tech energy-dispersive system. Oxide and silicate phases were analyzed at 20 kV acceleration voltage and 20 nA sample current (on brass). Natural minerals (albite, chromite, kaersutite, almandine, apatite, magnetite, pentlandite, biotite, rutile, rhodonite, galena) and pure metals were used as standards. Representative microprobe analyses are presented in Tables 1 and 2. Calculation of Fe^{3+}/Fe^{2+} in ilmenite was done using the method of *Droop* (1987).

Geological setting

Forster (1965) gave a first comprehensive picture of the geological setting in this part of the NE Bavarian Basement (Fig. 1). The major part of the study area is underlain by Moldanubian paragneisses composed of variable amounts of biotite, sillimanite, cordierite, quartz, garnet, and feldspar. Second in abundance are felsic igneous rocks of Late Carboniferous age, including aplites and pegmatites of different grain size and mineral composition. These igneous rocks are mainly located in the center and at the eastern edge of the study area. Along the western, southern and northern margins of this cluster of igneous rocks, swarms of quartz veins intersect the basement gneisses in NW-SE direction. Their morphological expression in the field, texture and mineralogy are similar to those of the "Great Bavarian

Fig. 2. Titanium placer minerals in continental environments – past and present **a** Subangular nigrine intergrown with quartz (nigrine type A). Location: Pflaumbach near Pleystein. **b** Angular complex ilmenite-rutile intergrowth of nigrine type A. Location: Pflaumbach near Pleystein. **c** Bed load deposit of subrounded grains of nigrine (black) disseminated between gravel of vein quartz (bright) and gneiss (dark gray) in a creek near Pleystein. **d** Subrounded to rounded grains of nigrine concentrated manually by panning in the field. Location near Pleystein

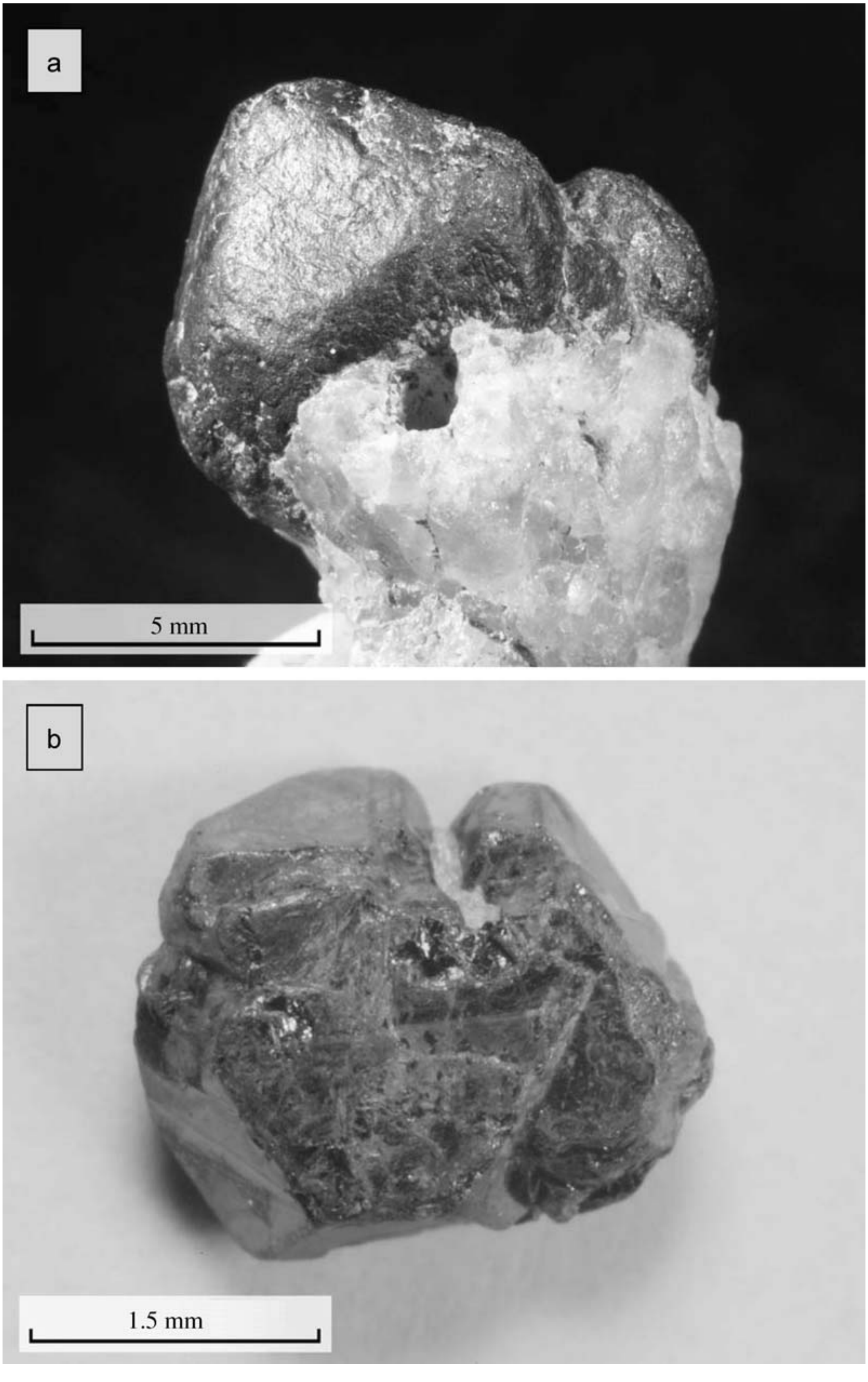
a
5 mm
b
1.5 mm

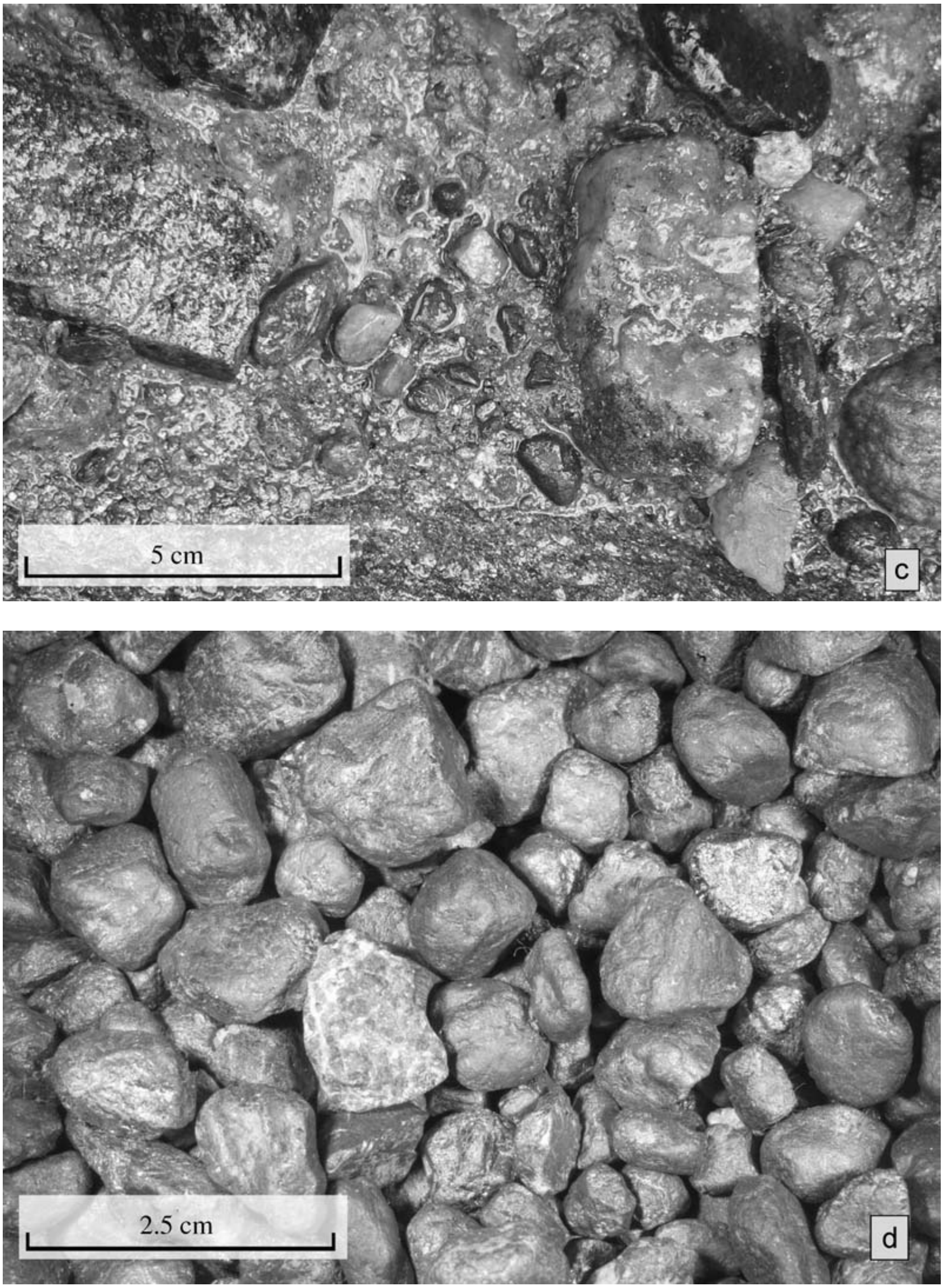

Fig. 2 (*continued*)

Quartz Reef'' (*Siebel* et al., 2005). Quartz veins are absent from the area intruded by the Late Variscan granites and shaped by the Cenozoic drainage system that gave host to the Ti placers under consideration.

Results

Mineralogy and textures of nigrine

In the following, three types of nigrine (A, B1, B2) found in placer deposits of NE Bavaria are presented (Fig. 2a–d). Type A comprises zoned grains consisting of a rutile core (host) and an ilmenite rim. Inclusions of wolframite are common. Rutile and ilmenite are intergrown crystallographically as flame-like ilmenite exsolutions in rutile and vice versa in a core-rim transition zone. Type B comprises grains of ilmenite hosting lamellae of niobian rutile. In subtype B1 rutile has exsolved Nb-bearing rutile lamellae, and the ilmenite has abundant hematite exsolutions and inclusions of ferrocolumbite and pyrochlore. In subtype B2, Nb-, Fe- and V-rich rutile exsolves directly from ilmenite. Another grain type, rutile C, is monomineralic but W-rich, lacking the complex intergrowth with ilmenite and any mineral inclusions observed in types A and B. Their characteristic textural and chemical peculiarities are summarized in Table 3.

Nigrine type A: Nigrine type A occurs in the placers as well rounded to rounded grains exceeding locally 10 mm in size. Optical examination under reflected light and the use of backscattered-electron images (BSE) reveals a complex intergrowth of twinned rutile which forms the core of the aggregates, with ilmenite forming a rim, up to 1.5 mm thick (Figs. 3a, b, 4a). Oriented lamellae of ilmenite are particularly abundant near the edge of the rutile core, and lamellae of rutile occur in the ilmenite rim. Wolframite and zircon are abundant inclusions and are restricted to the ilmenite rim. Very similar zoned grains of nigrine type A were found in the host rock outcrops around Pleystein (samples 7135, 7136; Table 3). These grains, 4–5 mm in size, are hosted by quartz, muscovite, orthoclase (with quartz-orthoclase symplectites), biotite and albite of much smaller grain size (<1 mm), with accessory Nb-bearing rutile, Mn-bearing ilmenite, Fe oxides, apatite, zircon and pyrrhotite.

Chemical profiles across the rutile-ilmenite aggregates show a complex behavior of major and minor elements (Fig. 5), which is most likely controlled by intragrain diffusion processes. In most grains, three different zones are distinguished: a rutile core zone, an inclusion-rich rutile-ilmenite transition zone (several 100 μm thick), and an ilmenite rim. The rutile core is characterized by constantly high TiO_2 (>96 wt.%), up to 1 wt.% V_2O_3 and Nb_2O_5, some FeO (up to 0.7 wt.%), and lower Mn, Mg, Cr, Ta and W. Concentrations of Nb are fairly constant within one grain, e.g., 0.8–1.0 wt.% Nb_2O_5 in the example depicted in Fig. 5 (Table 1, columns 11–12; Fig. 6), but may also display weak continuous zoning with concentrations increasing in the transition zone. Similar behavior is observed for Cr (reaching 0.3 wt.% Cr_2O_3 in the transition zone), V, Mg, W, Sc and Mg, whereas Fe and Nb are lower than in the core (Fig. 7). The ilmenite rim has quite constant Ti/Fe ratios, and carries Mn and Mg as significant impurities. Minor elements present in the rutile core, e.g., Cr, V, and Ta, are low or close to the detection limits in the ilmenite. Scandium (up to 0.04 wt.% Sc_2O_3) is concentrated in ilmenite compared to rutile. Nb_2O_5 decreases to almost zero in the transition zone and increases gradually to values as high as 0.4 wt.% in the outer ilmenite rim (Table 1, columns 1–2). Iron, V and Mg follow similar enrichment trends. Tiny rutile grains and lamellae in the rutile-ilmenite transition zone may contain up to 7 wt.% Nb_2O_5 as well as

Table 3. *Mineralogical and chemical composition (concentrations in wt.%) of nigrine aggregates and rutile type C from the NE Bavarian basement*

Sample	Type	Texture	Size mm	Rutile core			Rutile lamellae/grains			Ilmenite			Inclusions						Alteration	
				Nb_2O_5	V_2O_3	FeO	Nb_2O_5	V_2O_3	FeO	MnO	MgO	Nb_2O_5	hm-lam	Wolframite	Columbite	Pyrochlore	Zircon	Others	‘‘Pseudorutile’’	‘‘Leucoxene’’
7134/1	A	zoned rutile grain with ilmenite rim	11	0.8–1	0.7–1.0	0.2–6	1.1–7.4	1.0–2.0	0.5–2.9	1.1	0.5	<0.3		x					x	
7135	A	zoned rutile grain with ilmenite rim	5	0.5	0.7	0.4	3.3	1.2	2	1.7	0.2	0.1		x					x	
7136	A	zoned rutile grain with ilmenite lamellae and rim	4	0.3	0.8	0.5	1.1–3.5	0.8	1.1	1.8	0.3	0.1		x				sph, po		
7193/1	A	zoned rutile grain with ilmenite rim, strong alteration	8.4	0.1–0.8	0.4–0.8	0.3–0.7	1.4–5.8	0.8–1.6	0.5–2	4	0.05	0.14					x		x	x
7193/2	A	zoned rutile grain with thin ilmenite rim, flame-like ilm lamellae	6	0.4–0.8	0.7	0.3–0.4	n.a.			3	0.17	0.1								
7193/3	A	zoned rutile grain with thin ilmenite rim, flame-like ilm lamellae	6.4	1.1–1.4	0.7–1	0.4–0.7	to 6.5	1.4	2.9	2.5–2.8	0.15	0.1–0.2					x			
7193/4	A	zoned rutile grain with thick ilmenite rim, flame-like ilm lamellae	10	0.2–0.3	0.6–0.8	0.2–0.3	0.8	0.7	0.4	2.0–2.4	0.2	0.05–0.15		x					x	
7193/5	A	zoned rutile grain with thick ilmenite rim, flame-like ilm lamellae	7.2	0.5–0.7	0.6–0.8	0.3–0.4	to 10	to 2.1	to 4.8	2.0–3.7	0.2–0.3	0.1–0.3					x		x	
7193/6	A	zoned rutile grain with thin ilmenite rim, flame-like ilm lamellae	6	0.4–0.6	0.8–1.0	0.2–0.3	to 4	to 1.2	to 1.2	2.3–2.6	0.15	<0.1								
7167/4	A	rutile with ilmenite rim	0.4	0.96	0.9	0.6				3	0.03	0.09								
7134/2	B1	ilmenite-rutile intergrowth with complex exsolution features	6	0.3–0.4	0.5	0.4–0.8	1.5–8.6	0.5–0.7	1.0–4.2	2.4	<0.1	0.22	x		x	x		mt		
7194/1	B2	ilmenite grain with thin lamellae of Nb-rutile	3				18–21	2.6	6–7	1.5	0.25	0.3–0.5		x	x		x			

(*continued*)

Table 3 (*continued*)

Sample	Type	Texture	Size mm	Rutile core			Rutile lamellae/grains			Ilmenite			Inclusions						Alteration	
				Nb_2O_5	V_2O_3	FeO	Nb_2O_5	V_2O_3	FeO	MnO	MgO	Nb_2O_5	hm-lam	Wolframite	Columbite	Pyrochlore	Zircon	Others	‘‘Pseudorutile’’	‘‘Leucoxene’’
7194/2	B2	ilmenite grain with thin lamellae of Nb-rutile	2.5				13–15	>3	4–5	2.5	0.1	0.3–0.4		x			x		x	
7194/3	B2	altered rutile lamellae in ilmenite matrix	3				0.03–2.4	0.4–1.0	0.2–1.7	7–9	<0.05	0.12–0.15							x	x
7194/4	B2	ilmenite grain with thin lamellae of Nb-rutile, altered	3				1.9–10.2	0.8–1.6	0.6–3.5	2.3–2.5	0.1–0.4	0.1–0.25							x	
7167/5	B2	ilmenite grain with thin lamellae of rutile	0.5				3.2	1.1	1.5	3.5	0.05	0.02					x			
7167/7	B2	ilmenite grain with thin lamellae of rutile	0.4				4.1	1.4	1.5	3.5	0.05	0.06								
7167/2	C	rutile with exsolution lamellae of W-enriched rutile	0.5	0.15	0.6	0.5	0.3	1	2											

hm-lam Hematite lamellae; *sph* sphalerite; *po* pyrrhotite; *mt* magnetite; *x* present; *n.a.* not analyzed

Sample localities for placers: Pingermühle (Zottbach) (7134); Pflaumbach near Pleystein (7167); Zollgraben (7193); Iglasreuth, Tirschenreuther Waldnaab (7194)

Sample localities for bedrock: Weißenstein (7135); Steiniger Loh, NW Fahrenberg (7136)

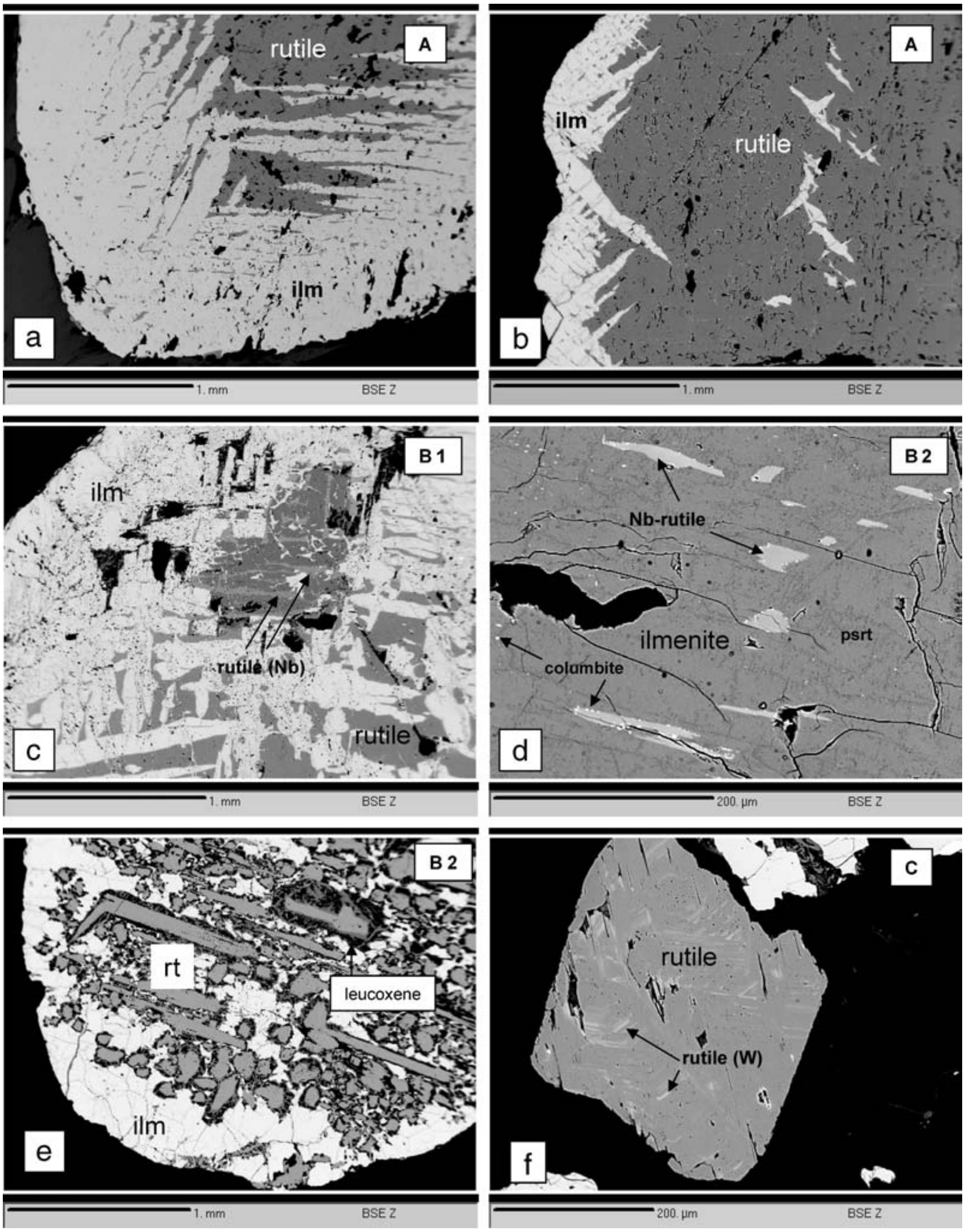

Fig. 3. Micrographs of nigrine types (Back-scattered electron images/BSE). **a** Rutile core with rim of ilmenite (ilm). Nigrine type A; sample 7135. **b** Oriented exsolution lamellae of ilmenite (ilm) in and near the edge of a rutile core. Nigrine type A; sample 7193/2. **c** Intergrowth of rutile (dark) and ilmenite (bright) in nigrine type B1. Subparallel wavy to discontinuous exsolution lamellae of Nb-enriched rutile are observed in matrix rutile; sample 7134/2. **d** Ilmenite with lamellae of niobian rutile in nigrine type B2. Surfaces of rutile are speckled with tiny crystals of columbite (white). Ilmenite is altered to pseudorutile (psrt), recognizable by its darker color in the BSE image; sample 7194/1. **e** Dendritic to graphic intergrowth of lath-shaped rutile and ilmenite in nigrine type B2. Ilmenite is altered to pseudorutile and to a Ti-rich phase (leucoxene) along the rutile surfaces; sample 7194/3. **f** Trellis-like patterns of W-enriched rutile exsolved from W-poor rutile; sample 7167/2

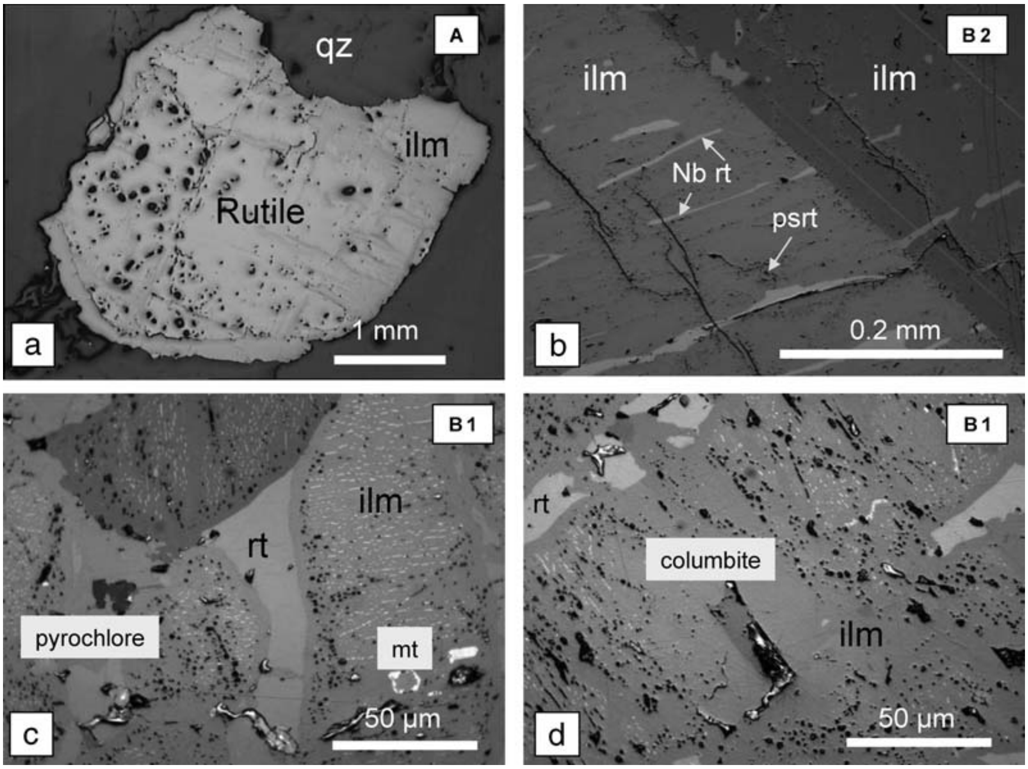

Fig. 4. Photomicrographs of nigrine grains taken in reflected light; all photos with one polar. **a** Nigrine type A: zoned rutile-ilmenite aggregate with attached bedrock (quartz-orthoclase-biotite); sample 7136. **b** Two individual ilmenite (ilm) crystals (pleochroic) with oriented lamellae of niobian rutile (Nb rt), and replaced by pseudorutile (grey phase along cracks). Nigrine type B2; sample 7194/2; oil immersion objective. **c** Ilmenite (ilm) with abundant hematite exsolution blebs (white) intergrown with rutile (rt); a few individual inclusions of magnetite (mt) and pyrochlore (dark). Nigrine type B1; sample 7134/2; oil immersion objective. **d** Large columbite (grey) included in ilmenite (ilm) with abundant hematite exsolution blebs (white), intergrown with rutile (rt). Nigrine type B1; sample 7134/2; oil immersion objective

elevated V_2O_3 (>2 wt.%), Cr_2O_3 (>0.6 wt.%), Ta_2O_5 (up to 0.4 wt.%), WO_3 (up to 2 wt.%) and FeO (up to 2.7 wt.%) (Table 1, columns 5–6).

Nigrine type B1: One well-rounded grain consists of a complex intergrowth of ilmenite and rutile (Fig. 3c), and inclusions of ferrocolumbite and pyrochlore (Fig. 4c, d). The core-rim zonation of rutile and ilmenite, as it was recognized in type A nigrine, is not as strongly developed in this type; for this reason, it is termed B1 nigrine. BSE images and microprobe analyses revealed needle-shaped discontinuous exsolution lamellae of Nb-enriched rutile (1.5–8.6 wt.% Nb_2O_5) within Nb-poor rutile (0.3–0.4 wt.% Nb_2O_5) (Figs. 3c, 6, Table 1, column 7); such Nb-rich areas cannot be distinguished from normal rutile in reflected light. The rutile areas also have crystallographically oriented, very thin lamellae of ilmenite, whereas the grainy ilmenite carries abundant hematite exsolution lamellae (Fig. 4c, d). Compared to other nigrine types, the ilmenite in type B1 has lower Ti contents, and elevated Nb and V concentrations (Table 1, column 3; Fig. 8).

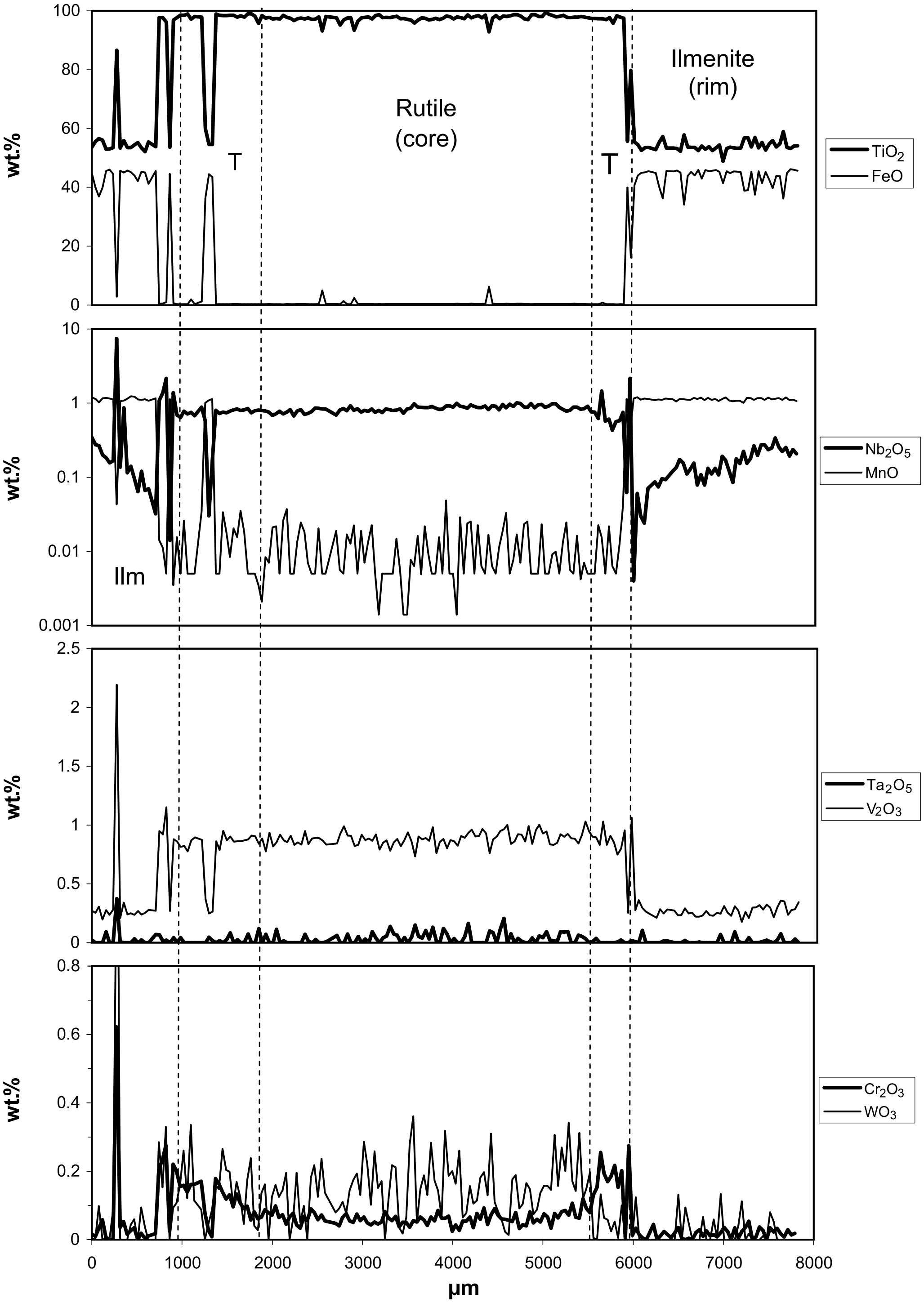

Fig. 5. Chemical transect across zoned nigrine grain (type A, sample 7134/1) consisting of a rutile core, ilmenite rims (ilm), and transition zones (T). Note the logarithmic scale for Nb and Mn. Spikes in the transition zone and the ilmenite rims are inclusions and lamellae of Nb-bearing rutile, and of ilmenite in the rutile phase, respectively

Nigrine type B2: Grains of nigrine B2 are smaller than those of B1 falling in the range 0.4–3 mm. They consist of an ilmenite host with oriented lamellae of rutile (Figs. 3d, e, 4b). The inclusion assemblage is dominated by wolframite, ferrocolumbite and zircon. Rutile occurs as ovoids randomly distributed in the ilmenite (Fig. 3e) or as lath-shaped inclusions in an oriented intergrowth with ilmenite (Figs. 3d, 4b). In some B2 nigrine grains, rutile and ilmenite are intergrown in a patchwork fashion resembling trellis-type lamellae. Ilmenite is replaced by a more Ti-rich alteration product (pseudorutile, Figs. 3d, 4b). Rutile lamellae in nigrine type B2 may be exceptionally rich in Nb, Fe, and V with up to 21 wt.% Nb_2O_5, 2.6 wt.% V_2O_3 and as much as 7 wt.% FeO (Figs. 6, 7; Table 1, columns 8–9, 13). The ilmenite carries MnO (1.5–9 wt.%) as a major impurity, and Nb_2O_5 may reach 0.4 wt.% (Table 1, column 4).

Rutile C: Aggregates of rutile C are similar in size to aggregates of nigrine A and B but different in composition (Fig. 3f). In BSE images two different phases may be distinguished in the rutile aggregate. Needles of W-rich rutile (5 wt.% WO_3) are encountered in a W-poor rutile host (Table 1, column 10).

Chemical composition of nigrine and rutile C aggregates

Rutile core: Rutile cores of nigrine aggregates are characterized by low, but consistent concentrations of Nb (up to 1.4 wt.% Nb_2O_5), V (up to 1 wt.% V_2O_3), Fe (up to 0.8 wt.% FeO), and Cr (up to 0.2 wt.% Cr_2O_3). The concentrations of Ta, Sc, W, Sn, Mn, Mg are mostly below the detection limit of the electron microprobe (Table 1, columns 11–13). Some grains show continuous zoning of V, Cr, Fe, V, W, and Nb with increasing values towards the rutile-ilmenite transition zone (Fig. 5).

Rutile and ilmenorutile lamellae: Lamellae and grains in the rutile-ilmenite transition zone of type A nigrine grains have considerably higher concentrations of impurities than the core rutile, reaching 10 wt.% Nb_2O_5, 2 wt.% V_2O_3 , 4.8 wt.% FeO, 0.6 wt.% Cr_2O_3, and 2.0 wt.% WO_3 (Table 1, columns 5–6). Lamellae in type B nigrine grains may contain exceptional contents of Nb_2O_5 (21 wt.%) and FeO (7 wt.%), as well as V_2O_3 (2.6 wt.%), Cr_2O_3 (0.7 wt.%) and 1.8 wt.% WO_3 (Table 1, columns 7–9). On the basis of four oxygen atoms, the trace element-rich niobian rutile has a formula of $(Ti_{1.46}Nb_{0.29}Fe_{0.18}V_{0.06})O_4$; thus, 25% of the metals are metals other than Ti. This "niobian rutile" corresponds to ilmenorutile [$(Ti,Nb,Fe)O_2$], which forms a solid-solution series with strüverite [$(Ti,Ta,Fe)O_2$] (*Černy* et al., 1981; *Černy* and *Ercit*, 1985; *Černy* et al., 1999). The negative correlation of Ti with other metals is illustrated for the lamellar inclusions in different nigrine types in Fig. 6, and compared to the more restricted composition of their respective rutile cores. The impurity elements Nb, Ta, Fe, V, Cr and W show reasonable to good positive correlations (Fig. 7). Cation totals normalized to 4 oxygens exceeding the ideal value of 2.0 (Table 1, columns 5–10) have been observed before, and are attributed either to oxygen deficiency ($Ti^{4+} \leftrightarrow 2Fe^{3+}$) or to $3Ti^{4+} \leftrightarrow Fe^{3+}$ substitution, or both (*Černy* et al., 1981).

Ilmenite: The composition of ilmenite in the nigrine aggregates varies in terms of Ti-Fe ratio and the concentrations of additional elements, especially of Mn and Mg. In most ilmenites analyzed, $Ti/(Ti + Fe)$ ranges from 0.5 to 0.53, extending to 0.57 in places (Fig. 8); only type B1 ilmenite is significantly

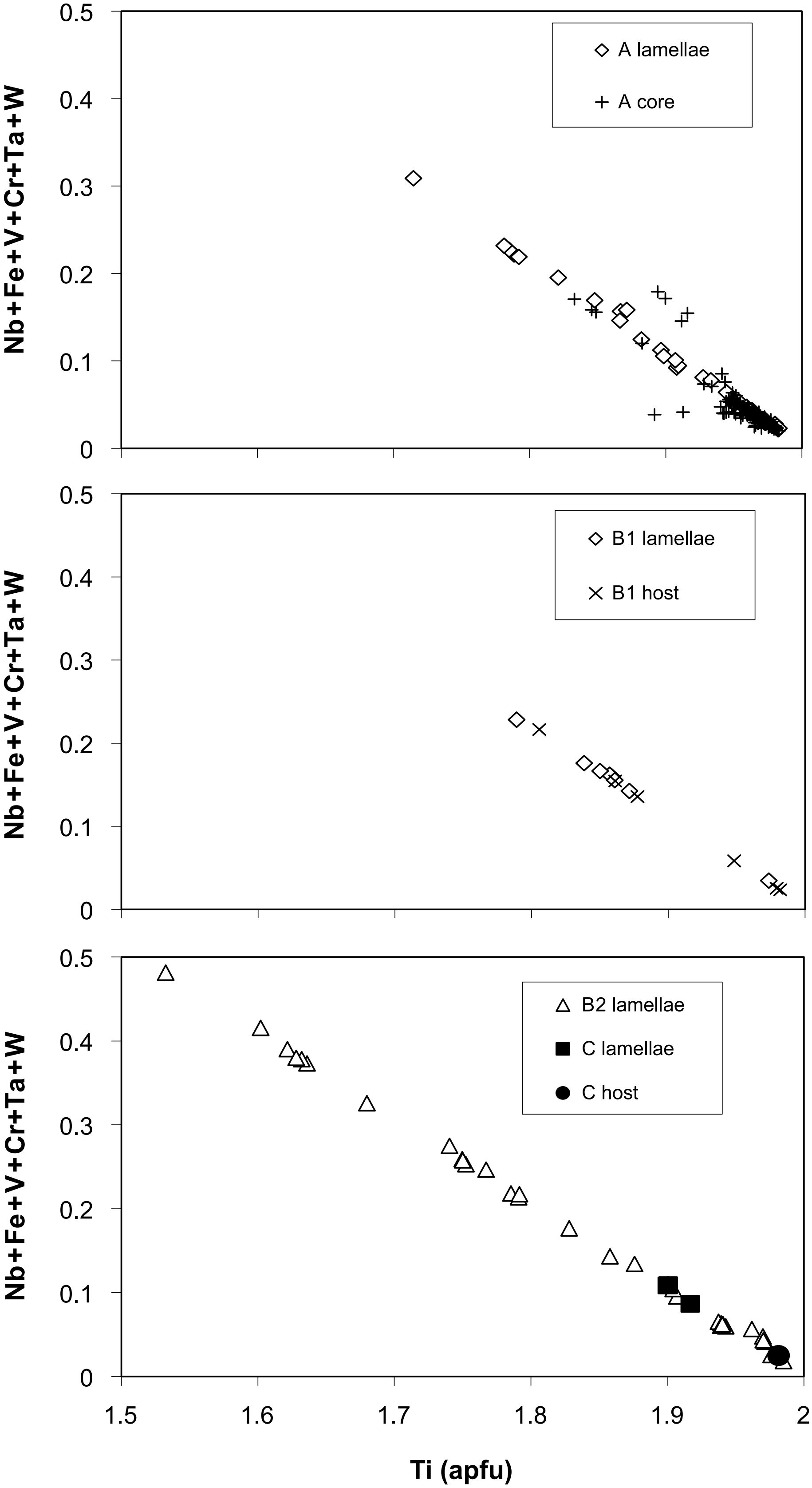
A lamellae
A core
B1 lamellae
B1 host
B2 lamellae
C lamellae
C host
Nb+Fe+V+Cr+Ta+W
Nb+Fe+V+Cr+Ta+W
Nb+Fe+V+Cr+Ta+W
0.5
0.4
0.3
0.2
0.1
0
1.5
1.6
1.7
1.8
1.9
2
Ti (apfu)

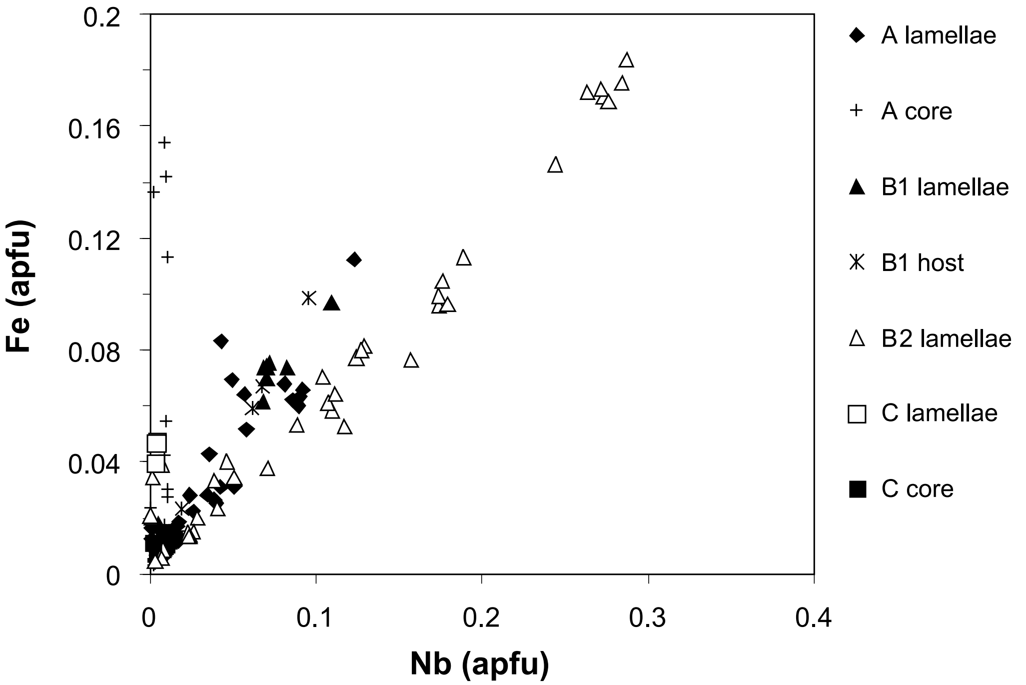

Fig. 7. Variation of Nb versus Fe in rutile lamellae and cores of nigrine grains in atoms per formula unit based on 4 oxygens

enriched in Fe, probably due to submicroscopic inclusions of hematite (Fig. 4c, d, Table 1, column 3). The intra-grain variation of the Ti-Fe ratio is high, probably due to alteration processes removing and oxidizing Fe (see later). The Mn concentrations in ilmenite are homogeneous within grains. Most grains have between 1 and 4 wt.% MnO, with only one B2 type grain having 8–9 wt.% MnO (Fig. 8). MgO concentrations are usually between 0.1 and 0.2 wt.%, and reach 0.4–0.6 wt.% in few types A and B2 grains only. The concentrations of those elements that are considerably enriched in rutile (Nb, V, Cr, W) are lower, but often detectable. Nb_2O_5, for example, reaches 0.5 wt.% in some type B2 grains. V_2O_3 is fairly constant at 0.2–0.4 wt.% in all grains (Table 1, columns 1–4).

Mineral inclusions in nigrine

Wolframite: Wolframite is a mineral common to types A and B nigrine, occurring as small (<10 µm) single-phase inclusions in ilmenite only. Based on the Fe/(Fe + Mn) ratios between 0.91 and 0.93, the mineral may be described as almost pure ferberite (Table 2, columns 3–4).

Zircon and sulfides: Zircon inclusions are ubiquitous in nigrine and were not analyzed in detail. Sphalerite and pyrrhotite are rare constituents, only identified under the microscope in nigrine type A2.

Fig. 6. Composition of rutile in nigrine grains, in atoms per formula unit (apfu) calculated to 4 oxygen atoms. Lamellae are distinguished from homogeneous cores in types A, B1, B2 and C

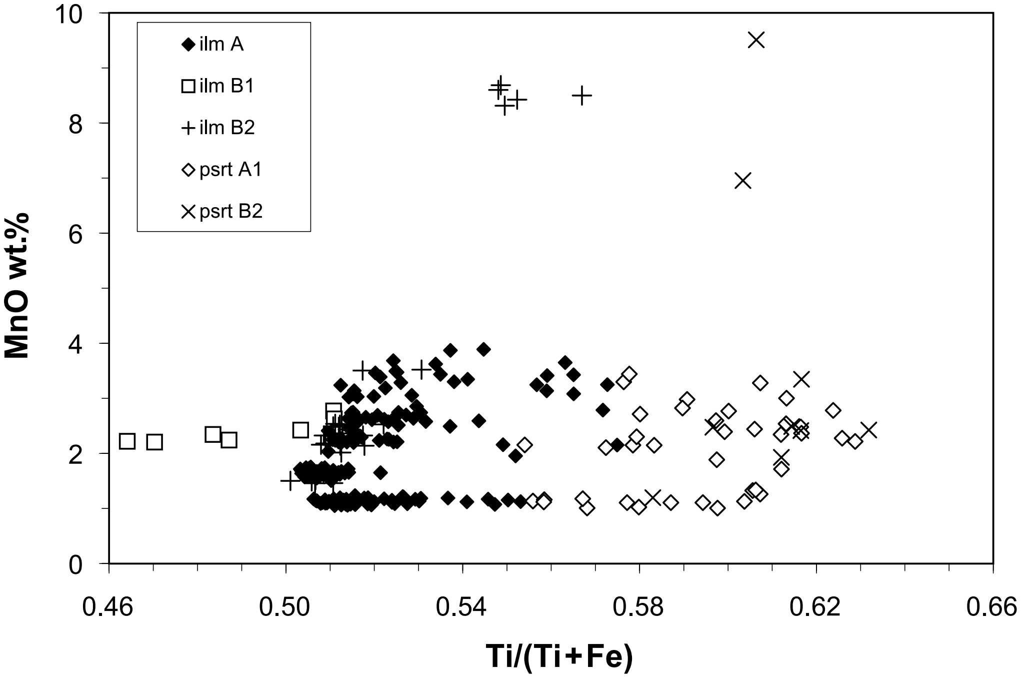

Fig. 8. Compositional variation of ilmenite (ilm) and pseudorutile (psrt) in four groups of nigrine grains. Pseudorutile as defined here is characterized by lower totals than ilmenite; the transition from ilmenite to pseudorutile is set at Ti/(Ti + Fe) values of 0.55

Ferrocolumbite: Single inclusions and aggregates of ferrocolumbite of the general formula (Fe,Mn)$(Nb,Ta)_2O_6$, up to 40 µm across (Fig. 4d), are restricted to types B1 and B2 nigrine. Within a given grain of nigrine, compositions are rather homogeneous, but differ slightly between grains. In type B1, ferrocolumbite is associated with pyrochlore-group minerals, and with wolframite in type B2. Weak zoning in some back-scatter electron images is due to slightly higher concentrations of Ta in cores compared to rims (e.g., 3.4 vs 3.0 wt.% Ta_2O_5). Ferrocolumbite in inclusions in nigrine aggregates are Nb- and Fe-rich, with $0.80 < Fe/(Fe + Mn) < 0.90$ and $0.97 < Nb/(Nb + Ta) < 0.99$ (Table 2, columns 1–2). Additional elements in significant concentrations are Sc (up to 2.5 wt.% Sc_2O_3), W (up to 3.2 wt.% WO_3), Sn (up to 0.5 wt.% SnO_2), Mg (up to 0.5 wt.% MgO) and Ca (up to 3.4 wt.% CaO). Vanadium, Cr, Al and Pb may occur in traces. The concentrations of TiO_2 range from 3 to 8 wt.%, but the effect of secondary fluorescence from surrounding ilmenite is not clear. Compared to ferrocolumbite included in type B1 nigrine, the ferrocolumbite from B2 nigrine is depleted in Nb and Mn but enriched in Ca, Ti and W. Iron-rich columbite is typically found in pegmatitic rocks poor in F and carrying, e.g., beryl (*Černy*, 1992).

Pyrochlore: Inclusions of the pyrochlore-group $[A_{2-m}B_2X_6[(O,OH,F) = Y]_{1-n}{}^{*}pH_2O$ (*Hogarth*, 1977)] are confined to ilmenite in type B1 nigrine where they form grains up to 40 µm in size that may be associated with columbite (Fig. 4c). They are chemically dominated by Nb and Ca, with minor Ta (up to 3.1 wt.% Ta_2O_5), Ti, W, Fe, and traces of V, Mn, Sn, Sc, Al, Na, U and Pb (Table 2, column 5). The chemical requirements to qualify for a member of the pyrochlore group, i.e. $Nb + Ta > 2Ti$ and $Nb > Ta$, are met. The calculated average formula of $Ca(Nb_{1.78}Ta_{0.04}Ti_{0.16}Fe^{3+}{}_{0.06})_2O_6$ is close to the aeschynite-type [(Ce,Ca,Fe,Th) $(Ti,Nb)_2(O,OH)_6$]. In the same host grain of ilmenite, betafite [$(Ca,U,Na)_2(Ti,Nb,Ta)_2(O,OH)_7$, *Nickel* and *Nichols*, 2004] was found as zoned grains up to 30 µm in size, having 29 wt.% UO_2 and an average formula of $(Ca_{1.1}Na_{0.2}U_{0.4})_{\Sigma 1.7}(Nb_{1.0}Ta_{0.1}Ti_{0.9})_{\Sigma 2.0}(O,OH)_7$ (Table 2, column 6). Betafite is replaced at the margin by a hitherto unknown phase. The results obtained from microprobe analysis point to a Nb–Ti–Ta-rich phase with minor concentrations of Fe, U, P, Al, Si, Ca, Pb, Sn, V and Mn (Table 2, column 7); taking into account the low totals, H_2O or $(OH)^-$ may be expected. Relative to betafite, Nb and Ta are enriched at the expense of Ca and U in the altered product. It might represent hydrated betafite.

Iron oxides: Magnetite inclusions are sporadically observed in the ilmenite phase of type B1 nigrine (Fig. 4c) only, occurring as subhedral to euhedral crystals up to 10 µm in size. According to microprobe analyses they contain up to 3.2 wt.% TiO_2 (Table 2, column 8), corresponding to a low-Ti titanomagnetite. Ilmenite displays frequent, almost submicroscopic hematite exsolution lamellae only in nigrine type B1 (Fig. 4c, d).

Alteration products of nigrine

"Hydroilmenite", "leached ilmenite", pseudorutile: Ilmenite is commonly replaced by a more Ti-rich phase along the edges and fissures, commonly in a dendritic pattern, in nigrine types A and B (Figs. 3d, e, 4b, d). By definition, $Ti/(Ti + Fe)$ ratios between 0.6 and 0.7 qualify Ti–Fe compounds as pseudorutile (*Grey* et al., 1994), while minerals with lower ratios are rather called "hydroilmenite" (*Frost* et al., 1983), a name not validated by the IMA. *Mücke* and *Bhadra Chaudhuri* (1991) introduced the term "leached ilmenite", and *Chernet* (1999a) used "pseudoilmenite" to describe a leaching product intermediate between ilmenite and pseudorutile showing similar color and anisotropy than ilmenite. In reflected light and using oil immersion, the alteration products are characterized by grayish color and a reflectance lower than ilmenite (Fig. 4b–d); compared to strongly bireflecting and anisotropic ilmenite, pleochroism and anisotropic effects are inconspicuous or absent. Microprobe analyses give low totals in the range of 94 to 99 wt.% and $Ti/(Ti + Fe)$ ratios between 0.55 and 0.63 (Fig. 8). The analyses shown in Table 2 (columns 11–13) represent average values with most individual analyses ranging from 56 to 63 wt.% TiO_2 and 32 to 45 wt.% Fe_2O_3; some analyses having up to 76 wt.% TiO_2 at 23 wt.% Fe_2O_3 are transitional to leucoxene. The MnO and MgO contents are similar to their ilmenite precursor phases (1–9 wt.% MnO, 0.1–0.6 wt.% MgO, <0.5 wt.% Nb_2O_5, 0.2–0.4 wt.% V_2O_3), although Mn appears to decrease slightly with increasing Ti, i.e. with advancing alteration (Fig. 8). On the basis of formula calculations using 9 oxygen and 5 cations, the iron in altered ilmenite grains is almost completely oxidized to Fe^{3+}, whereas the host ilmenites contain very little Fe^{3+}. The low totals can be attributed to introduction of some H_2O or $(OH)^-$ (*Mücke* and *Bhadra Chaudhuri*, 1991). The mechanism of ilmenite hydration is not documented in the samples, but it may firmly be assumed that water was introduced along fractures.

Leucoxene (?): An alteration phase similar in texture but different in composition to pseudorutile was exclusively found associated with rutile of some types A and B nigrines (Fig. 3e). The chemical composition points to a Ti-rich phase (76 wt.% TiO_2) with appreciable concentrations of impurities, e.g. 2.0–2.5 wt.% FeO, 6.1–8.5 wt.% Al_2O_3, 3.5–4.1 wt.% P_2O_5, and subordinate amounts of V, Si and Ca. Totals in the range 90 to 95 wt.% suggest considerable incorporation of H_2O or the $(OH)^-$ complex (Table 2, columns 9–10). The phase may be considered a special type of leucoxene, i.e. submicroscopic intergrowths of TiO_2, Al-rich phosphates and silicates.

Discussion

The source of nigrine and W-enriched rutile

Accessory ilmenite and rutile in gneisses of the NE Bavarian basement are of much smaller grain size than the Ti aggregates in the stream sediments around Pleystein (*Propach*, 1969). Moreover, single grains of ilmenite or rutile are more widespread in basement rocks than aggregates of both minerals as they were found in grains of nigrine A and B from the alluvial-fluvial sediments. Rutile grains from metapelitic and mafic rocks usually carry 0.1–0.3 wt.% and 0–0.18 wt.% Nb, respectively (*Zack* et al., 2004). This level is well below the Nb contents analyzed from rutile of the nigrine placer deposits. Therefore metamorphic rocks may definitely be ruled out as a source for nigrine and highly differentiated igneous rocks are most likely the source for the nigrine and rutile.

During the collisional stage of the Variscan orogeny several pegmatites were emplaced near Hagendorf and Pleystein (Fig. 1), containing Li phosphates, Nb-, Ta-, U-oxides and numerous other rare element minerals (*Teuscher* and *Weinelt*, 1972; *Forster* and *Kummer*, 1974; *Strunz* et al., 1975; *Tennyson*, 1981; *Mücke*, 1987; *Mücke* et al., 1990).

The Late Variscan pegmatites between Pleystein and Hagendorf are Nb-selective with Nb contents exceeding the Ta contents by some orders of magnitude (*Teuscher* and *Weinelt*, 1972). Such high Nb/Ta ratios were observed in the rutile component of nigrine grains, and in columbite from type-B nigrine. Niobium becomes a marker element, connecting the pegmatite-borne mineralizations with the detrital nigrine in the placer deposits. Titanium minerals, common to the placer deposits, are rare constituents of the mineral assemblage of the Hagendorf pegmatite province. In the upper portions at Hagendorf, above the 90 m level, an older pegmatite carrying abundant potassic feldspar is intruded by a younger quartz-enriched pegmatitic root zone below (*Uebel*, 1975). *Mücke* (2000) subdivided the mineralization at the lower level in two paragenetic associations: (1) pyrrhotite stage, and (2) iron-oxide stage. Ilmenite and rutile are rare inclusions in magnetite. Minerals encountered in the older alkali feldspar-quartz pegmatites at an intermediate mining level or near surface have no equivalent among the secondary mineral assemblage in the placer deposits, with the exception of ferrocolumbite. Feldspar and the phosphate minerals bearing divalent Fe and Mn from the older pegmatite are very susceptible to chemical weathering and, hence, decomposed during post-Variscan times when a subtropical climate provoked a pervasive chemical weathering and erosion capped the NE Bavarian basement to great depth (*Dill*, 1995). Rutile and nigrine are more resistant to these conditions of chemical weathering than feldspar and phosphate minerals and, locally, acted as a shelter for less resistant minerals such as ferberite and pyrochlore. The placer deposits around Pleystein mirror the evolution of the Late Variscan pegmatites at the western edge of the Bohemian Massif. Different stages of the pegmatite evolution may be deduced from the composition and texture of the different types of nigrine A and B as well as from the W-enriched rutile C: (1) low-Nb quartz vein stage (A), (2) high-Nb pegmatite stage (B), (3) high-W stage (C). Furthermore, there is a wide range of compositional changes on transport or storage that left their imprints on grains of nigrine and rutile and allow for another subdivision of alteration processes, namely a (4) ferric-ferrous titanium alteration stage, and a (5) phosphate-titanium alteration stage.

Pegmatite evolution reflected by detrital nigrine and rutile

Low-niobium quartz vein stage: The nigrine grains are characterized by a specific element assemblage (in decreasing order of abundance: Ti, Fe, V, Nb, Mn, W, Mg, Cr, Ta, Sc, Sn, U) that reflects both their source as well as the process of crystallization. If we assume that the zoned and exsolved nigrine grains once formed from homogeneous grains, chemical traverses (e.g., Fig. 5) may be used to estimate their original composition. For zoned nigrine grains of type A this simplified approach yields the following ranges: 75–85 wt.% TiO_2, 13–17 wt.% FeO, 0.5–0.7 wt.% V_2O_3, 0.4–0.9 wt.% MnO, 0.2–0.6 wt.% Nb_2O_5, 0.03–0.11 wt.% WO_3, 0.07–0.18 wt.% MgO, 0.02–0.03 wt.% Ta_2O_5. The atomic ratios are 4–6 for Ti/Fe, 13–38 for Fe/Mn and 17–38 for Nb/Ta. Nigrine grains of type B1 are too heterogeneous for estimation of the original composition. Ilmenite grains with exsolution lamellae of niobian rutile or ilmenorutile (nigrine B2) will have lower Ti/Fe ratios than type A grains, and higher Nb concentrations. For comparison, recalculation of the original composition of niobian rutile from the McGuire pegmatite, Colorado, gave (simplified) $(Ti_{2.3}Nb_{0.8}Ta_{0.1}Fe^{3+}{}_{0.4}Fe^{2+}{}_{0.4})_4O_8$ or 20 mol% of Nb component (*Černy* et al., 1999). There, an original rutile has completely exsolved into Nb-bearing pseudorutile I, that broke down to Nb-rich pseudorutile II embedded in Nb-Fe bearing "ferropseudobrookite", and later exsolved into niobian rutile, titanian ferrocolumbite and ilmenite.

The primary source of type-A nigrine lies in the NW-oriented quartz veins (Figs. 1, 2a, b). Mineral inclusions, textural features and the chemical signature between placer- and quartz-hosted nigrine are almost identical. *Brenan* et al. (1994) measured rutile from high-pressure quartz veins that contained only 50 ppm Nb and *Zack* et al. (2002) investigated rutile from Disentis, Switzerland, with ca. 150 ppm Nb, but with substantial amounts of Cr (1200 ppm Cr). Low Nb concentrations are explained by a low capacity of fluids for transporting high field strength elements (*Xiong* et al., 2005).

The ilmenite exsolution in rutile and the rim around rutile are controlled by the ferric/ferrous iron ratio and the f_{O2}. The buffering reaction is as follows: $2\ Fe_2O_3 + 4\ TiO_2 \leftrightarrow 4\ FeTiO_3 + O_2$ (*Zhao* et al., 1998). At present we cannot provide fully quantitative data on the Fe^{3+}/Fe^{2+} ratio due to the limitations placed by the EMP analyses. However, formula calculations on the basis of 4 cations and

6 oxygens indicate very low Fe^{3+}/Fe^{2+} ratios in all ilmenites except those of type B1, where the contribution of Fe^{3+} to total Fe averages to 9%. In types A and B2 nigrines, Fe^{3+}/Fe^{tot} averages to only 0.2 to 0.6. An indirect way to get an idea on the f_{O2} may be provided by minerals included in A-type nigrine. Apart from high-field strength elements Zr, Nb and Ta which are compatible in rutile, there are polyvalent elements like W which are very sensitive to the oxygen fugacity (*Klemme* et al., 2005). Although the W content of A-type nigrine is rather low, wolframite was identified, attesting to a rather moderate oxygen fugacity during this stage of quartz-rutile-ilmenite mineralization. Oscillation of elements during core-margin transition in A-type nigrine, shown by the chemical transect in Fig. 5 is interpreted in terms of a strong diffusion process, which is a common process in the pegmatite stage. Despite some uncertainties about the precise composition of the original phase, the entire process of exsolution or differentiation was less prominent during the low-niobium quartz vein stage than during the stage discussed in the following chapter. The low-niobium quartz vein stage is representative of the younger pegmatite transitional into the barren vein quartz.

High-niobium pegmatite stage: For the high-niobium nigrine of type B, no equivalent source rock was identified close-by. The "rune-like" or "graphic" intergrowth in nigrine is fostered by the epitactic relations between the original rutile and ilmenite and similar in appearance to the graphic feldspar-quartz intergrowth known from the core-margin zone of the host K-feldspar-quartz pegmatites of the Hagendorf province. Some of the B-type nigrine inclusions resemble Nb-Ti-U mineralization in the core zones of the late Variscan pegmatites of the Hagendorf pegmatite province. Therefore the term pegmatite stage is justified. Type-B placer mineralization is similar to the mineralization recorded from the 115 m-mining level of the feldspar pegmatite upward. Exsolution and separation of Ti phases prograded and diffusion processes at the rutile-ilmenite boundaries are more pronounced than during the previous quartz stage, generating true niobian rutile intergrown with ilmenite enriched in Mn and containing inclusions of columbite and, in places, pyrochlore-group minerals.

The tungsten contents in columbite inclusions, although extremely variable, are very high with as much as 8.89 wt.% WO_3. They resemble W contents reported from the Vezná pegmatite, Czech Republic and the McGuire pegmatite, USA (*Černy* et al., 1999, 2000). Wolframite included by rutile of type B nigrine corroborates correlation of type-B nigrine from the placer with the sulfide stage in the pegmatite which developed at approximately 450 °C (*Mücke* et al., 1990).

Based upon the Fe/(Fe + Mn) ratios ranging from 0.82 to 0.89 and the Nb/(Nb + Ta) ratios of 0.98 this titanian ferrocolumbite is typical of columbites from beryl-bearing F-impoverished pegmatites (*Černy*, 1992). In general, these Nb-Ta oxides exhibit decreasing Nb/Ta ratios with progressive fractionation (*Aleksandrov* 1963; *Linnen* and *Keppler*, 1997). Columbite included in type-B nigrine is still more selective for Nb than equivalent columbites reported by *Forster* (1965) from the nearby pegmatite (56.5 wt.% Nb and 22.8 wt.% Ta). The rather high Nb/Ta ratio determined from columbite inclusions in type-B nigrine suggests that the host environment for these nigrine-columbite mineral aggregates was less strongly fractionated than the adjacent Hagendorf pegmatite that was taken for reference.

Columbite is replaced by pyrochlore in type-B nigrine. A mineral assemblage, composed of Nb-rutile, columbite, aeschynite and pyrochlore, similar to that from B-type nigrine occurs in some of the veins associated with the Bayan Obo iron-rare earth-niobium deposits, Inner Mongolia, China (*Drew* et al., 1990). In the Bayan Obo deposit, this mineral association represents the waning stages of the main mineralizing system, and is related to a Hercynian heating event. The preponderance of W of type-B placer nigrine which has no match in the pegmatites is considered as a mineralization transitional from the pegmatitic into the hydrothermal stages. It is considered as a stage distal to the older Hagendorf pegmatite, *sensu Uebel* (1975). *Linnen* and *Keppler* (1997) have shown that Ta/Nb solubility in the melt is an important factor for separation of Nb and Ta. During type-B nigrine mineralization in the source area, the differentiation of a granitic melt has no longer played a crucial role.

High-tungsten stage: Detrital type-C rutile stands out among the Ti compounds in the study area by its high WO_3 contents (up to 5 wt.%). Rutile grains in alluvial tin concentrates, mostly from the Western Tin Belt from Peninsular Malaysia contain tungsten in the range 0.5–1.0 wt.% WO_3 (*Hassan*, 1994). Rutile associated with biotite in the Potrerillos granite, Argentine, formed during post-magmatic alteration, ranges up to 7.14% WO_3 (*Sardi*, 2003). High-W rutile C is held to be of (pneumatolytic)-hydrothermal origin. Its comparatively low Nb contents resemble what has been observed in type-A nigrine samples from the NW-SE striking quartz veins in the western part of the study area. Conclusively, the high-W rutile represents a transitional stage between the barren quartz veins proximal to the Late Variscan pegmatite province and the wolframite-(gold) quartz veins at Neualbenreuth far off that pegmatitic zone near the Czech-German border (*Dill*, 1985, 1989).

Supergene alteration of nigrine

Ferric-ferrous titanium alteration stage: Pseudorutile and leucoxene are the products of ilmenite alteration under fluctuating redox conditions. Dendritic pseudorutile alters the host ilmenite under oxidizing conditions (Figs. 3d, e, 4c, d). The question, if this conversion of bivalent into trivalent iron went on under hypogene or supergene conditions is difficult to answer (*Anand* and *Gilkes*, 1985). Pseudorutile and leucoxene replacing ilmenite along fissures and cracks took place simultaneously in a slightly acidic environment near the water table of an old peneplain during the Cenozoic or even Late Mesozoic (*Dill*, 1995). Judging by the preponderance of pseudorutile over leucoxene oxidizing conditions prevailed most of the time.

Phosphate-titanium alteration stage: Primary phosphates such as apatite, triphylite or triplite are common in the pegmatites of the Hagendorf pegmatite province. They were attributed to the group of primary phosphates (*Forster*, 1965). The Al-Fe-P-bearing "leucoxene" compound may be ascribed to a supergene process during which Fe and Al were remobilized under slightly acidic and permanently oxidizing conditions. Saprolites which may contain such an aluminum-phosphate-sulfate mineralization formed throughout the Cenozoic and Late Mesozoic on various types of bedrock of the NE Bavarian Basement, examples of which have also been found among the secondary phosphates in the Hagendorf province (*Dill*, 2001).

Conclusions

Detrital grains of nigrine and associated W-enriched rutile in placer deposits in the Hagendorf pegmatite province provide clear evidence of a pegmatitic to hydrothermal derivation. Nigrine A is the detrital mirror image of the quartzose root zone of the younger pegmatite. Nigrine B is representative of the marginal facies of the older pegmatite stage found at an intermediate level in the in Late Variscan pegmatites.

Rutile C, albeit its paragenetic position could not precisely be fixed in the mineral succession, is the missing link between the pegmatitic nigrine mineralization mentioned above and the skarn-type scheelite mineralization nearby (*Jakob*, 1979) and hydrothermal wolframite-quartz veins (*Dill*, 1985, 1989). Nigrine grains underwent supergene alteration near and above the water table of an ancient palaeoaquifer.

Nigrine and rutile being abnormally rich in W may lead exploration geologists to rare-element pegmatites and may also be useful for sedimentologists who want to learn more about the source areas of heavy minerals in clastic sediments.

Acknowledgments

We are indebted to *J. Lodziak* who conducted the microprobe analyses. We express our gratitude to *A. Mücke* and an anonymous referee for their valuable comments on the manuscript during review of this paper.

References

Aleksandrov VB (1963) Isomorphism of cations in titaniferous tantalo-niobates of composition AB_2X_6. Dokl Akad Nauk 153: 672–675 (English translation 129–131)

Anand RR, Gilkes RJ (1985) Some alumina and silica in weathered ilmenite grains is present in clay minerals – a response to *Frost* et al. (1983). Mineral Mag 49: 141–145

Bloomfield K (1958) The geology of the Port Herald area. Nyasaland Protectorate Geological Survey Department Bulletin 9: 1–76

Brenan M, Shaw HF, Phinney DL, Ryerson FJ (1994) Rutile-aqueous fluid partitioning of Nb, Ta, H, Zr, U and Th: implications for high field strength element depletions in island-arc basalts. Earth Planet Sci Lett 128: 327–339

Černy P (1992) Geochemical and petrogenetic features of mineralization in rare-element granitic pegmatites in the light of current research. Appl Geochem 7: 393–416

Černy P, Ercit TS (1985) Some recent advances in the mineralogy and geochemistry of Nb and Ta in rare-element granitic pegmatites. Bull Minéral 108: 499–532

Černy P, Chapman R, Simmons WB, Chackowsky E (1999) Niobian rutile from the McGuire granitic pegmatite, Park County, Colorado: Solid solution, exsolution, and oxidation. Amer Mineral 84: 754–763

Černy P, Novák M, Chapman R, Masau M (2000) Two-stage exsolution of a titanium (Sc, Fe^{3+})(Nb,Ta)O_4 phase in Norwegian niobian rutile. Can Mineral 38: 907–913

Černy P, Paul BJ, Hawthorne FC, Chapman R (1981) A niobian rutile-disordered columbite intergrowth from the Huron Claim pegmatite, southeastern Manitoba. Can Mineral 19: 541–548

Chernet T (1999a) Applied mineralogical studies of the Koivusaarenneva ilmenite deposit, Kälviä, Western Finland, with special emphasis on the altered part of the ore. Chron Rech Min 535: 19–28

Chernet T (1999b) Effect of mineralogy and texture in the TiO_2 pigment production process of the Tellnes ilmenite concentrate. Mineral Petrol 67: 21–32

Clark (1993) Hey's mineral index. Mineral species, varieties and synonyms, 3rd edn. Chapman & Hall

Coakley GJ, Mobbs PM (2001) The mineral industry of Malawi. Mineral industries of Africa and the Middle East, US Geol. Survey Minerals Yearbook 1998–2003: 29.1–29.2

Dill HG (1985) Die Vererzung am Westrand der Böhmischen Masse. – Metallogenese in einer ensialischen Orogenzone. Geol Jb D 73: 3–461

Dill HG (1989) Metallogenetic and geodynamic evolution in the Central European Variscides – A pre-well site study for the German Continental Deep Drilling Programme. Ore Geol Rev 4: 279–304

Dill HG (1995) Heavy mineral response to the progradation of an alluvial fan: implication concerning unroofing of source area, chemical weathering, and paleo-relief (Upper Cretaceous Parkstein fan complex/SE Germany). Sed Geol 95: 39–56

Dill HG (1998) A review of heavy minerals in clastic sediments with case studies from the alluvial-fan through the nearshore-marine environments. Earth Sci Rev 45: 103–132

Dill HG (2001) The geology of aluminium phosphates and sulphates of the alunite supergoup: A review. Earth Sci Rev 53: 25–93

Drew LJ, Qingrun M, Weijun S (1990) The Bayan Obo iron – rare earth – niobium deposits, Inner Mongolia, China. Lithos 26: 46–65

Droop GTR (1987) A general equation for estimating Fe^{3+} concentrations in ferromagnesian silicates and oxides from microprobe analysis using stoichiometric criteria. Mineral Mag 51: 431–435

Forster A (1965) Erläuterungen zur Geologischen Karte von Bayern 1:25000 Blatt Vohenstrauß/Frankenreuth. GLA München, 174 pp

Forster A, Kummer R (1974) The pegmatites in the area of Pleystein-Hagendorf/North Eastern Bavaria. Fortschr Mineral 52: 89–99

Frost MT, Grey IE, Harrowfield IR, Mason K (1983) The dependence of alumina and silica contents on the extent of alteration of weathered ilmenites from Western Australia. Mineral Mag 47: 201–208

Grey IE, Watts JA, Bayliss P (1994) Mineralogical nomenclature: pseudorutile revalidated and neotype given. Mineral Mag 58: 597–600

Hassan WF (1994) Geochemistry and mineralogy of Ta-Nb rutile from Peninsular Malaysia. J Southeast Asian Earth Sci 10: 11–23

Hogarth D (1977) Classification and nomenclature of pyrochlore group. Amer Mineral 62: 403–410

Jakob H (1979) Neue Scheelit-Vorkommen in Nordostbayern. Der Aufschluss 30: 187–192

Klemme S, Prowatke S, Hametner K, Günther D (2005) Partitioning of trace elements between rutile and silicate melts: implications for subduction zones. Geochim Cosmochim Acta 69: 2361–2371

Linnen RL, Keppler H (1997) Columbite solubility in granitic melts: Consequences for the enrichment and fractionation of Nb and Ta in the Earth's crust. Contrib Mineral Petrol 128: 213–227

Morton AC (1984) Stability of detrital HM in Tertiary sandstones from the North Sea basin. Clay Miner 19: 287–308

Morton AC (1985) Heavy-minerals in provenance studies. In: *Zuffa GG* (ed), Provenance of arenites. NATO ASI Ser C 148: 249–277

Mücke A (1987) Sekundäre Phosphatmineralien (Perloffit, Brasilianit, Mineralien der Kingsmountit-Gruppe) sowie Brochantit und die Zwieselit-Muschketoffit-Stipnomelan-Pyrosmalith-Paragenese der 115-m-Sohle des Hagendorfer Pegmatits. Aufschluss 38: 5–28

Mücke A (2000) Die Erzmineralien und deren Paragenesen im Pegmatit von Hagendorf-Süd, Oberpfalz. Aufschluss 51: 11–24

Mücke A, Keck E, Haase J (1990) Die genetische Entwicklung des Pegmatits von Hagendorf-Süd/Oberpfalz. Aufschluss 41: 33–51

Mücke A, Bhadra Chaudhuri JN (1991) The continuous alteration of ilmenite through pseudorutile to leucoxene. Ore Geol Rev 6: 25–44

Nickel E, Nichols M (2004) Mineral names, redefinitions & discreditations passed by the CNMMN of the IMA. http://www.materialsdata.com

Propach G (1969) Über Ilmenit und Rutil als Einschlüsse im Biotit eines redwitzitischen Gabbros. Geol Bavarica 60: 150–155

Ramdohr P (1975) Die Erzminerale und ihre Verwachsungen: Akademie-Verlag, Berlin, 1277 pp

Raufuss W (1973) Struktur, Schwermineralführung, Genese und Bergbau der sedimentären Rutil-Lagerstätten in Sierra Leone (Westafrika). Geol Jb D 5: 1–52

Sardi FG (2003) Composición química de la betafita, ilmenita, rutilo y rabdofano del yacimiento W-Mo ≪Badillo≫, Angulos, Argentina. Revista de la asociación geológica argentina 58: 1–18

Siebel W, Ulrich Blaha U, Chen F, Rohrmüller J (2005) Geochronology and geochemistry of a dyke-host rock association and implications for the formation of the Bavarian Pfahl shear zone, Bohemian Massif. Int J Earth Sci 94: 8–23

Strübel G, Zimmer SH (1982) Lexikon der Mineralogie. Enke Verlag Stuttgart

Strunz H, Forster A, Tennyson Ch (1975) Die Pegmatite in der nördlichen Oberpfalz. Aufschluss Sonderband 26: 117–189

Strunz V (1961) Nigrinfunde bei Pleystein. Aufschluss 1961: 30

Tennyson C (1981) Zur Mineralogie der Pegmatite des Bayerischen Waldes. Aufschluss 32: 49–73

Teuscher EO, Weinelt W (1972) Die Metallogenese im Raum Spessart-Fichtelgebirge-Oberpfälzer Wald-Bayerischer Wald. Geol Bavarica 65: 5–73

Uebel PJ (1975) Platznahme und Genese des Pegmatits von Hagendorf-Süd. N Jahrb Mineral Mh 1975: 318–332

Xiong XL, Adam J, Green TH (2005) Rutile stability and rutile/melt HFSE partitioning during partial melting of hydrous basalt: Implications for TTG genesis. Chem Geol 218: 339–359

Zack T, Kronz A, Foley SF, Rivers T (2002) Trace element abundances in rutiles from eclogites and associated garnet mica schists. Chem Geol 184: 97–122

Zack T, von Eynatten H, Kronz A (2004) Rutile geochemistry and its potential use in quantitative provenance studies. Sed Geol 171: 37–58

Zhao DG, Essene EJ, Zhang YX (1998) An oxygen barometer for rutile-ilmenite assemblages: oxidation state of metasomatic agents in the mantle. Earth Planet Sci Lett 166: 27–37

Authors' addresses: *H. G. Dill* (corresponding author, e-mail: dill@bgr.de), *F. Melcher*, Federal Institute for Geosciences and Natural Resources, P. O. Box 510163, 30631 Hannover, Germany; *M. Füßl*, A.-v.-Humboldt-Str. 4, 92711 Parkstein, Germany; *B. Weber*, Bürgermeister-Knorr Str. 8, 92637 Weiden i.d.OPf., Germany